Circulation
JOURNAL OF THE AMERICAN HEART ASSOCIATION

Real-Time Magnetic Resonance Imaging-Guided Endovascular Recanalization of Chronic Total Arterial Occlusion in a Swine Model

Amish N. Raval, Parag V. Karmarkar, Michael A. Guttman, Cengizhan Ozturk, Smita Sampath, Ranil DeSilva, Ronnier J. Aviles, Minnan Xu, Victor J. Wright, William H. Schenke, Ozgur Kocaturk, Alexander J. Dick, Venkatesh K. Raman, Ergin Atalar, Elliot R. McVeigh and Robert J. Lederman

Circulation published online Feb 20, 2006;
DOI: 10.1161/CIRCULATIONAHA.105.586727
Circulation is published by the American Heart Association. 7272 Greenville Avenue, Dallas, TX 72514
 Print ISSN: 0009-7322. Online ISSN: 1524-4539

Real-Time Magnetic Resonance Imaging–Guided Endovascular Recanalization of Chronic Total Arterial Occlusion in a Swine Model

Amish N. Raval, MD; Parag V. Karmarkar, MSc; Michael A. Guttman, MSc; Cengizhan Ozturk, MD, PhD; Smita Sampath, PhD; Ranil DeSilva, MBBS, PhD; Ronnier J. Aviles, MD; Minnan Xu, BS; Victor J. Wright, BS; William H. Schenke, BS; Ozgur Kocaturk, MSc; Alexander J. Dick, MD; Venkatesh K. Raman, MD; Ergin Atalar, PhD; Elliot R. McVeigh, PhD; Robert J. Lederman, MD

Background—Endovascular recanalization (guidewire traversal) of peripheral artery chronic total occlusion (CTO) can be challenging. X-ray angiography resolves CTO poorly. Virtually "blind" device advancement during x-ray–guided interventions can lead to procedure failure, perforation, and hemorrhage. Alternatively, MRI may delineate the artery within the occluded segment to enhance procedural safety and success. We hypothesized that real-time MRI (rtMRI)–guided CTO recanalization can be accomplished in an animal model.

Methods and Results—Carotid artery CTO was created by balloon injury in 19 lipid-overfed swine. After 6 to 8 weeks, 2 underwent direct necropsy analysis for histology, 3 underwent primary x-ray–guided CTO recanalization attempts, and the remaining 14 underwent rtMRI-guided recanalization attempts in a 1.5-T interventional MRI system. Real-time MRI intervention used custom CTO catheters and guidewires that incorporated MRI receiver antennae to enhance device visibility. The mean length of the occluded segments was 13.3±1.6 cm. The rtMRI-guided CTO recanalization was successful in 11 of 14 swine and in only 1 of 3 swine with the use of x-ray alone. After unsuccessful rtMRI (n=3), x-ray–guided attempts were also unsuccessful.

Conclusions—Recanalization of long CTO is entirely feasible with the use of rtMRI guidance. Low-profile clinical-grade devices will be required to translate this experience to humans. **(*Circulation*. 2006;113:1101-1107.)**

Key Words: angioplasty ■ catheterization ■ magnetic resonance imaging ■ occlusion ■ peripheral vascular disease

Chronic total occlusion (CTO) of peripheral arteries can cause disabling intermittent claudication or critical limb ischemia. Surgical revascularization offers symptom relief and limb salvage in eligible patients; however, perioperative morbidity, lengthy hospital stay, and slow functional recovery limit wider application.[1,2] Endovascular techniques are appealing because they offer prompt return of function and require neither general anesthesia nor extended hospital stay. However, endovascular recanalization of long, tortuous, occluded peripheral arteries remains challenging and risky, and therefore surgical or conservative management is typically recommended.[1]

Editorial p 1053
Clinical Perspective p 1107

X-ray fluoroscopic angiography with radiocontrast identifies the occluded inflow artery and possibly collateral-dependent outflow beyond the occlusion but cannot discriminate CTO arterial wall and lumen. In these cases, the entire occluded arterial segment remains invisible to the operator. Virtually "blind" device manipulation risks procedural failure and arterial perforation. Furthermore, ionizing radiation and nephrotoxic contrast exposure may become excessive during lengthy CTO recanalization procedures.

MRI can image the entire peripheral artery occlusion, including arterial wall, lumen content, and adjacent structures, without ionizing radiation or iodinated radiocontrast. Advances in rapid imaging, combined with development of catheter devices visible under MRI, have made real-time MRI (rtMRI)–guided therapeutic interventions feasible.[3–19] We hypothesize that rtMRI can guide catheter navigation within an occluded artery and that combined CTO recanalization and percutaneous transluminal angioplasty can be conducted en-

Received September 29, 2005; revision received December 13, 2005; accepted December 19, 2005.

From the Cardiovascular Branch (A.N.R., P.V.K., C.O., R.D., R.J.A., V.J.W., W.H.S., O.K., A.J.D., V.K.R., R.J.L.) and the Laboratory of Cardiac Energetics (M.A.G., S.S., E.R.M.), Division of Intramural Research, National Heart, Lung, and Blood Institute, National Institutes of Health, Bethesda, Md; Cardiovascular Section, Department of Medicine, University of Wisconsin, Madison (A.N.R.); and Department of Radiology, The Johns Hopkins University, Baltimore, Md (P.V.K., M.X., E.A.).

The online-only Data Supplement, which contains an Appendix, is available at http://circ.ahajournals.org/cgi/content/full/CIRCULATIONAHA.105.586727/DC1.

Correspondence to Robert J. Lederman, MD, Cardiovascular Branch, Division of Intramural Research, National Heart, Lung, and Blood Institute, National Institutes of Health, Building 10, Room 2c713, MSC 1538, Bethesda, MD 20892-1538. E-mail lederman@nih.gov

Circulation **is available at http://www.circulationaha.org** **DOI: 10.1161/CIRCULATIONAHA.105.586727**

tirely under rtMRI guidance with the use of custom MRI-visible devices in a swine model.

Methods

Balloon Injury Model

Animal protocols were approved by the National Heart, Lung, and Blood Institute Animal Care and Use Committee. National Institutes of Health miniswine (mean weight, 50±12 kg) were fed a 2% high-cholesterol diet for 1 week before CTO model creation and thereafter until recanalization was attempted 6 to 8 weeks later. After transfemoral access, an angioplasty balloon (Agiltrac, Guidant) sized 1.5 to 2 times artery diameter was positioned in the mid left carotid artery (LCA), inflated to nominal pressure, and rapidly withdrawn up to 6 times. Contrast-enhanced MR angiography (CEMRA) was performed at 2 weeks to confirm CTO. If the LCA remained patent (n=4), balloon injury was repeated.

Histology was performed on 2 uninstrumented CTO arteries 8 weeks after balloon injury. Formalin-fixed, paraffin-embedded, transverse sections (4 μm) were taken at 5-mm intervals along the artery length and stained with hematoxylin and eosin and Masson's trichrome.

Interventional MRI Suite

Procedures were performed in a previously described combined x-ray/MRI interventional suite (Axiom Artis/1.5-T Sonata, Siemens).[20] In-room hemodynamics, scan control, and rendered images were displayed with the use of shielded LCD projectors. Optical microphones (Phone-Or) and filtered headsets (Magnacoustics) permitted staff communication.

Digital subtraction x-ray and CEMRA of the arch and great vessels were performed immediately before and after intervention. Typical parameters (repetition time [TR] [ms]/echo time [TE] [ms]/flip angle [FA] [degrees]/bandwidth [Hz per pixel]/voxel size [VOX] [mm]) were as follows: TR/TE/FA/bandwidth/VOX=3.7/1.4/25/375/0.3×0.5×2, slab 300×244×128 mm. Real-time steady state free precession (rtSSFP) and 2D T1-weighted (T1w) spin echo axial images representing key anatomic planes were stored for uninterrupted retrieval during the intervention. Typical parameters were as follows: rtSSFP: TR/TE/FA/bandwidth/VOX=3.5/1.7/45/975/1.0×1.4×4; T1w: TR/TE/FA/bandwidth/VOX=800/12/180/130/0.5×0.5×3, 2 averages.

During rapid device manipulation in the aortic arch, rtSSFP frame rate was accelerated 3:1 with the use of echo sharing, wherein image data are interleaved over adjacent frames. Saturation prepulses suppressed background tissue to better visualize inflation of balloons filled with gadopentetate dimeglumine (0.8% Gd-DTPA, Magnevist, Berlex) and selective intra-arterial angiography (2.4% Gd-DTPA). Uninterrupted real-time subtraction angiography was achieved by displaying the difference between maximum intensity projections in time before and after the injection. Voxel size was reduced to increase spatial resolution, and temporal image filtering (averaging) was applied to improve signal-to-noise ratio (SNR) during slow device advancement within the CTO. Multiple oblique slices could be acquired simultaneously, repositioned interactively, and individually disabled and enabled as desired. Custom scan features allowed adjustment of pulse sequence, reconstruction, and display parameters without scan interruption. Finally, signals from separate device antennae could be independently displayed along their entire length, color-highlighted, and combined in real time with anatomic images from surface coils.

Interventional Devices

Active devices were prepared and tested in our laboratory. The intent was to create devices that were conspicuous along their entire length, including the tip.

Custom MRI Active CTO Support Catheter

Distal 1-cm microcoils were mounted on 6F ×100-cm angled, tapered, custom tungsten-braided catheters (Minnesota MedTec).

Figure 1. Custom active CTO guidewire telescoped within custom active CTO support catheter.

Coil signals are transmitted along the catheter shaft under insulating polyimide. Tuning, matching, and decoupling circuitry were attached at the proximal hub to prevent heating during MRI. The device was connected to a separate MR scanner receiver channel so that device-related images could be displayed in color.

Custom MRI Active CTO Guidewire

Consecutive gold-silver-gold–plated nitinol core wires were inserted within nitinol hypotubes, separated by polymer insulation. Closely wound MP35N (cobalt-chromium alloy) microcoils were attached distally to add wire flexibility, and 2.5-cm distal microcoils enhanced MRI receiver sensitivity at the tip. The final receiver-coil guidewire was 0.032 inch×155 cm, straight, and stiff. The proximal end of the guidewire had detachable connectors, permitting catheter exchange (Figure 1).

Custom Active Flexible "Workhorse" Guidewire

Flexible-tip nitinol guidewires (Nitrex, ev3, 0.032 inch×155 cm) were altered to serve as active, "loopless" design[21] receiver coils that were visible along their entire length. These were used as "workhorse" wires to safely deliver the CTO catheter to the origin of the occluded carotid artery.

Delivery Sheath

10F delivery sheaths (Fast Cath, St Jude; Brite Tip, Cordis) were trimmed to 75 cm. Stainless steel MRI markers (1 mm×0.014 inch) were bonded to the sheath tip, creating passive markers (discrete signal void) during MRI.

Device Testing

MRI heating tests (Appendix) were performed on CTO support catheters and guidewires with the use of previously described methods.[22,23]

rtMRI-Guided CTO Recanalization

The primary study end point was successful traversal of occluded arteries from their patent origins to their patent outflow regions. The secondary study end point was restoration of antegrade flow by adjunctive balloon angioplasty.

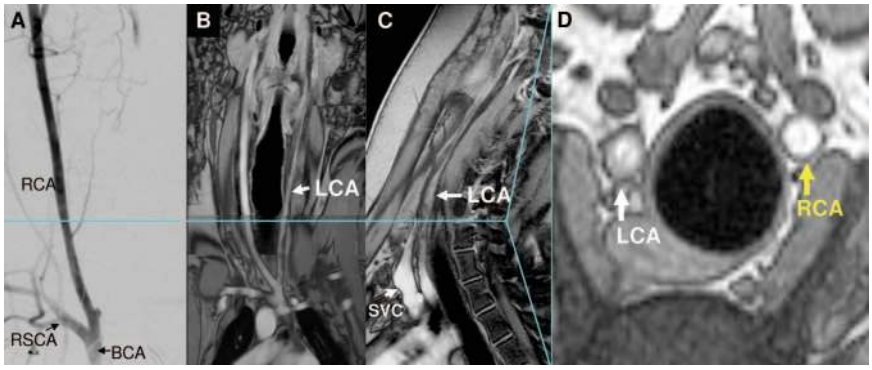

Figure 2. Baseline imaging of CTO lesions. A, Anteroposterior projection subtraction x-ray demonstrating "invisible" long LCA occlusion with distal reconstitution. Multislice T1w spin echo composite clearly demonstrates the entire occluded LCA in the coronal (B), sagittal (C), and axial (D) views. Linear dissection in the LCA is evident in the axial slice at this level (blue line). RCA indicates right carotid artery; RSCA, right subclavian artery; BCA, brachiocephalic artery; and SVC, superior vena cava.

Animals were pretreated with aspirin 325 mg and clopidogrel 300 mg. Intravenous heparin 100 U/kg bolus was given initially and supplemented with 50 U/kg every 2 hours. After sheath insertion, the active CTO support catheter was navigated to the brachiocephalic artery over the active floppy guidewire and positioned proximal to the occluded LCA. The floppy wire was exchanged for the active CTO wire. The CTO guidewire and catheter were steered intraluminally through the CTO with the use of multislice rtMRI. Two parallel slices orthogonal to the CTO artery centerline were used to ensure an intraluminal device course. One slice tracked the wire tip, and the second was advanced ahead of the wire tip, providing a target for the operator. Once the CTO was traversed, a 260-cm polytetrafluoroethylene guidewire (Glidewire, Terumo) was used to exchange the CTO guide catheter for a 100-mm-long peripheral angioplasty balloon sized 1:1 to the artery wall. After several balloon inflations with 5 mmol/L Gd-DTPA, selective angiography was performed with the use of 5 mL of 10 mmol/L Gd-DTPA. Intra-arterial nitroglycerin 200 to 400 μg was administered as needed to treat spasm.

Comparative X-Ray–Guided Recanalization of CTO Model

X-ray–guided recanalization was attempted in 3 swine by experienced interventionists to assess the suitability and procedural difficulty of the CTO model. Contemporary techniques and devices were used (Shinobi 0.014 inch, Cordis; Cross-It 0.010 to 0.014 inch, Guidant; Glidewire Straight Stiff and Super-Stiff 0.035 inch; 4F Glidecath, Terumo). Each attempt used high-performance x-ray imaging (Artis FC, Siemens) with 13-cm field of view, 15 frames per second, appropriate collimation, and at least 60 minutes of fluoroscopy. In 3 additional swine, after unsuccessful MRI-guided recanalization, x-ray–guided recanalization also was attempted.

Statistics and Analysis

Continuous variables were reported as mean±SD and were compared with a 2-tailed Student *t* test (Excel 2003, Microsoft). Discrete variables (procedure success) were compared by Fisher exact test.[24] The authors had full access to the data and take responsibility for its integrity. All authors have read and agree to the manuscript as written.

Results

Device Heating Tests

No significant heating was observed in phantom experiments during MRI of active CTO support catheters and guidewires (Appendix).

CTO Model Geometry and Histopathology

Native LCA diameter by x-ray was 4.6±0.7 mm before balloon injury, measured 70 mm cranial to the carotid bifurcation. Immediate preintervention CTO diameter (T1w) at this level and CTO length (CEMRA) were 4.7±1.3 and 133±16 mm, respectively. By comparison, the contralateral carotid artery diameter (T1w) at this level, the CTO minimal luminal diameter (T1w), and CTO maximal external wall diameter (T1w) were 5.0±0.7, 3.1±1.3, and 6.7±1.2 mm, respectively. These measurements suggest zones of positive (outward) and negative (inward) remodeling in this swine CTO model and are consistent with histology. MRI identified the entire CTO artery wall endoluminal and external boundaries and occasional proximal dissection flaps resulting from initial balloon injury (Figure 2). Histology of the explanted, naive CTO arteries revealed dense luminal collagen deposition, disrupted intima, microchannels, and distal organized thrombus (Figure 3).

rtMRI-Guided Recanalization

The primary end point, rtMRI-guided CTO recanalization, was achieved in 11 of 14 animals. The shaft profile and tips of the active devices were conspicuous while navigating the aorta and brachiocephalic arteries (Figure 4). The occluded artery walls and active interventional devices were easily visualized under MRI (Figure 5). Multiplanar imaging facilitated continuous assessment of device-anatomic relationships, enabling intraluminal device traversal. Mean time to wire traversal was 55±22 minutes (spread, 25 to 99 minutes), with an observed learning curve between the first and last third of interventions performed (69±23 versus 34±7 minutes; $P=0.048$). After balloon angioplasty, real-time selective MRA demonstrated brisk antegrade flow in 6 of 11 of those successfully recanalized with a guidewire (Figure 6). Gross necropsy of all successfully recanalized animals revealed mild artery thickening with no extramural hematoma (Figure 7) and appeared similar to the uninstrumented CTO lesions.

In 3 of 14 animals, the active guidewire would not advance beyond the proximal one third of the occluded segment despite an apparently intraluminal trajectory. After careful MRI interrogation to rule out any adverse sequelae such as hematoma, x-ray–guided attempts in all 3 were similarly unsuccessful.

In 2 of 11 successfully recanalized under rtMRI, antegrade blood flow was not achieved despite intra-arterial nitroglycerin and several prolonged balloon inflations because of refractory recoil, spasm, and unavailability of suitable stents. Intraluminal position was confirmed by selective real-time MR and x-ray angiography through the wire port of balloons positioned distal to the lesion.

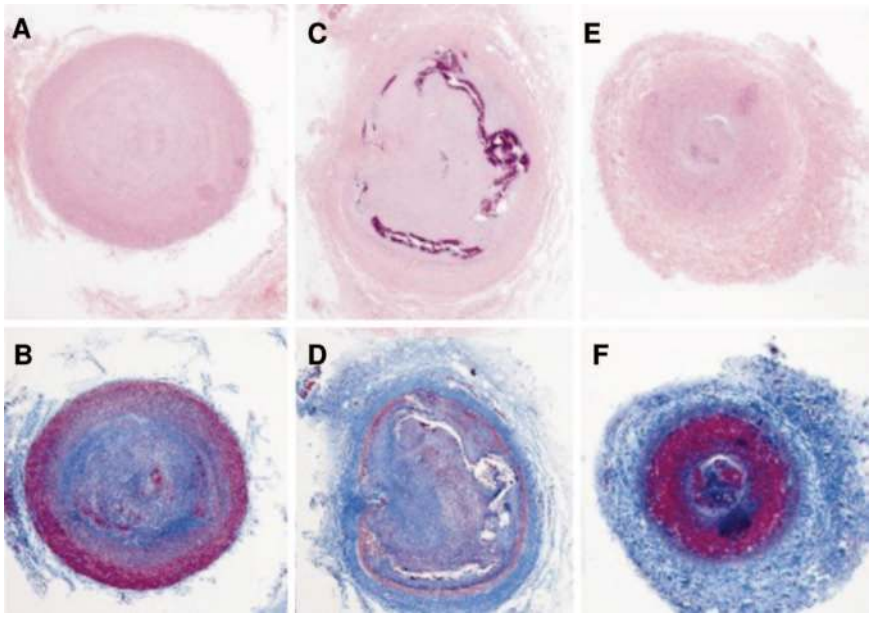

Figure 3. Representative histopathology sections; magnification ×4. Proximal (A and B), mid (C and D), and distal (E and F) transverse sections of CTO artery stained with hematoxylin and eosin (top) and trichrome (bottom). The central lumen is filled with collagen (pink in A, C, E; blue in B, D, F), disrupted intima with cellular infiltration (purple in C), and non-dispersed microchannels (C, D). Distal section ≈80 cm distal to bifurcation has intact intima and organized thrombus (red in F).

Homemade active CTO support catheters would not advance over active CTO guidewires that successfully traversed the occlusions in 3 of 11, preventing balloon exchange and subsequent angioplasty. In 1 of these 3 (the very first experimental animal), overaggressive attempts at advancing the active catheter over the wire resulted in clear real-time visualization of extraluminal CTO wire exit followed by extravascular hematoma accumulation. This complication was immediately recognized in rtMRI, and the procedure was aborted.

Comparative X-Ray–Guided Recanalization

Primary x-ray–guided CTO recanalization was successful in only 1 of 3 different animals attempted (requiring 45 minutes of fluoroscopy time). Crossover x-ray recanalization was also attempted in 3 of 14 animals after unsuccessful recanalization under rtMRI; none were successful. When these were combined, 1 of 6 x-ray–guided procedures were successful.

Successful CTO recanalization was more likely (79% versus 17%; $P=0.02$) during rtMRI attempts (11 of 14) compared with all x-ray–guided attempts (1 of 6). During extended primary x-ray recanalization attempts, wire exit caused contrast extravasation in one animal, and dissection was associated with lethal mediastinal hematoma in another.

rtMRI Enhancements

Subtraction real-time MRA improved visibility of intra-arterial Gd-DTPA injections compared with saturation preparation alone (Figure 6E and 6F). We increased spatial resolution by reducing the voxel size, but this degraded the SNR. We used temporal image filtering (averaging) to improve this reduced SNR during periods of slow device motion.

Discussion

Percutaneous peripheral artery CTO intervention can be highly challenging, time-consuming, and risky. Failure rates for iliac and femoropopliteal CTO are 3% to 36%[25–33] and 12% to 25%,[34,35] respectively. Novel alternative devices and techniques have had varied success for coronary and peripheral artery CTO recanalization, although to date none have prevailed clinically.[7,36–43]

This experience demonstrates successful wholly rtMRI-guided endovascular recanalization of long and challenging CTO with the use of custom devices in a suitable animal

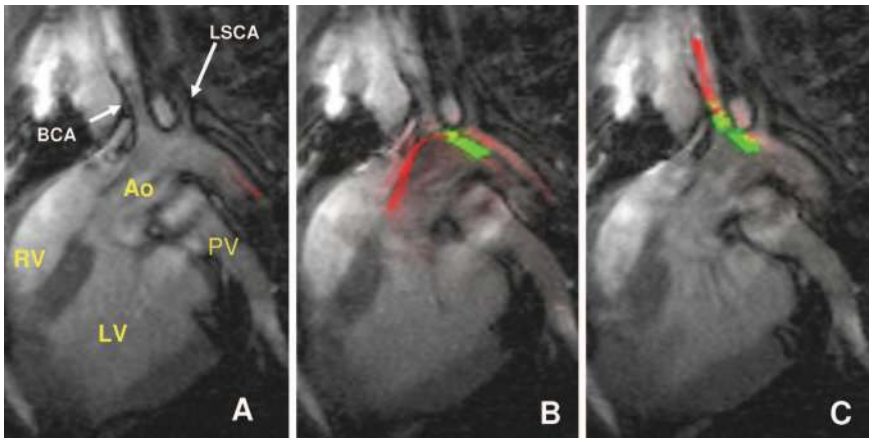

Figure 4. Positioning devices under rtMRI to begin CTO attempt. A, Active wire (red) entering descending aortic arch (Ao). B, The leading active wire is positioned safely in ascending aorta (Ao), and the active catheter (green) follows. C, Active wire and subsequently catheter are easily steered into brachiocephalic artery (BCA). LSCA indicates left subclavian artery; LV, left ventricle; and PV, pulmonary vein.

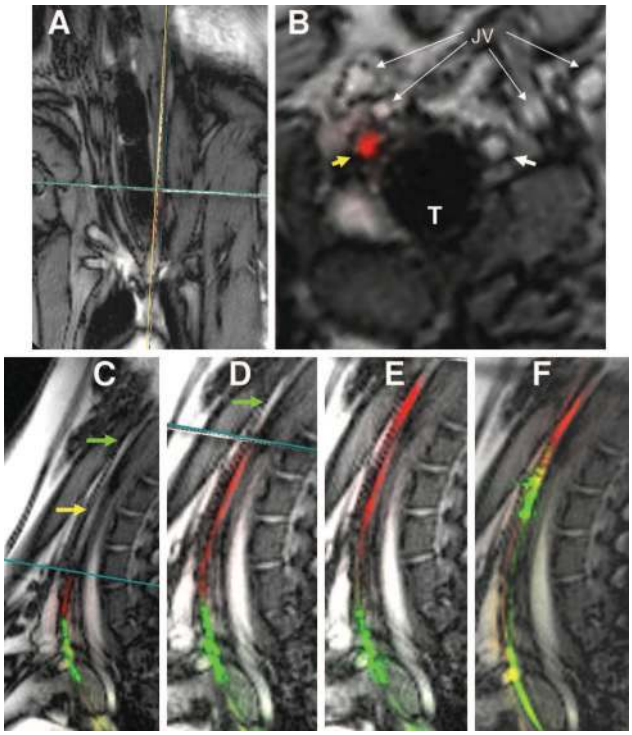

Figure 5. Traversing CTO with active guidewire and catheter. A, Real-time, interleaved, multiplanar MRI of coronal, sagittal, and transverse slices through occluded LCA. B, Transverse slice demonstrates right carotid artery (white arrow) and occluded LCA (yellow arrow). The active CTO wire tip (red) is seen entirely within the LCA lumen. C, Sagittal view of the occluded LCA (yellow arrow). The active wire (red) and catheter (green) are visualized proximally in the occluded LCA. The transverse slice (B) is continually translated cranially in advance of the CTO wire tip. D, The active wire is advanced through the remaining CTO into the patent distal LCA. E, The active catheter is tracked over the fixed wire into the distal patent LCA. F, Angioplasty balloon 5×100 mm inflated with dilute Gd-DTPA over active delivery wire (green). T indicates trachea; JV, external and internal jugular veins.

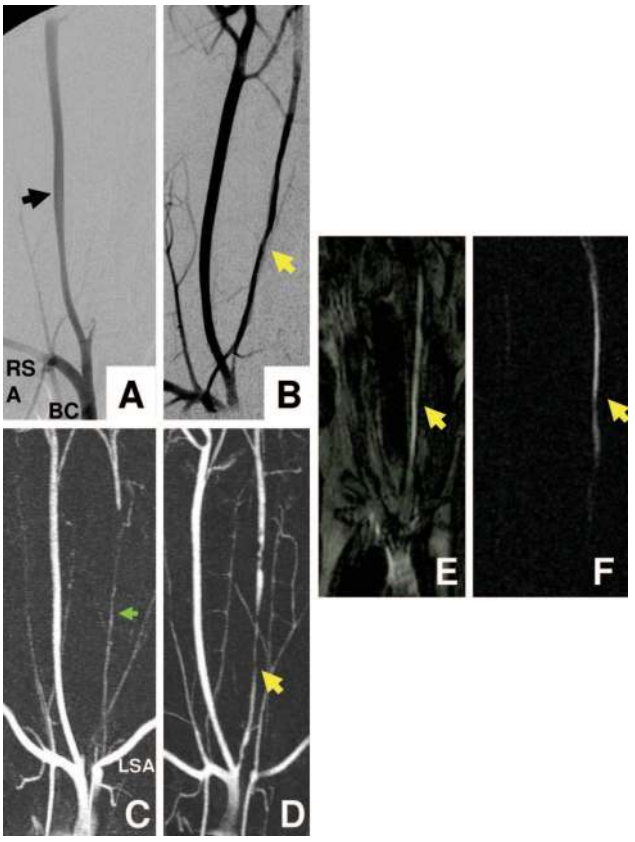

Figure 6. Multimodal angiography before and after CTO recanalization. A and B, Preintervention and postintervention anteroposterior projection subtraction x-ray demonstrates right carotid artery (black arrow) and patent postintervention LCA CTO (yellow arrow). C and D, Preintervention and postintervention CEMRA in the anteroposterior projection. Preintervention, the distal artery reconstitutes via cerebral collateral circulation with contribution from the left vertebral artery (green arrow) arising from the left subclavian artery (LSA). E and F, Selective real-time angiography gives immediate confirmation of successful recanalization into the patent LCA (yellow arrows) with saturation prepulse applied (E) and with better contrast with subtraction maximal intensity over time projection (F).

model. In this model, MRI was successful in 79% of attempts with the use of homemade devices and in 17% of all x-ray attempts with the use of higher-performance commercial devices.

The model CTO artery diameter and length resemble long (albeit rigid) human iliofemoral artery occlusions. These lesions would be considered TransAtlantic Inter-Society Consensus (TASC) type D, or best suited for surgical rather than endovascular recanalization.[1] Unlike x-ray, MRI delineates the occluded artery walls, permitting truly image-guided wire navigation. Custom "active" MRI CTO devices prove conspicuous and distinct from adjacent tissues. Procedure duration declined throughout this experience because of a "learning" phenomenon.

Device conspicuity, simultaneous display of multiple real-time imaging slices, and uninterrupted interactive features contributed to procedural success. Real-time selective MRA techniques with small volumes of dilute Gd-DTPA confirmed artery patency. This work represents an advance because a broad assortment of imaging and device features are fully integrated to support complex and completely rtMRI-guided vascular interventions.

Long conductive devices may heat significantly during MRI radiofrequency excitation and pose a safety concern. The custom active devices used here are appropriately tuned, matched, and decoupled and do not heat during scanning in a suitable test phantom (Appendix).

Our CTO model differs from tortuous, lipid, and calcium-rich atherosclerotic human iliofemoral disease. Severe arterial recoil and spasm prevented antegrade flow (n=2) or guiding catheter traversal (n=3) despite successful wire recanalization. The lesions were sufficiently long and challenging for a feasibility experiment. Of note, x-ray–guided recanalization attempts were less successful, even though they used higher-performance commercial clinical devices. Indeed, MRI guidance offers the potential to visualize the entire occluded segment and luminal boundaries, particularly in severely tortuous lesions often found in human peripheral CTO.

This experience adds to that of other published reports of rtMRI-guided procedures that traverse anatomic boundaries such as transjugular intrahepatic portosystemic shunt[14,44] and

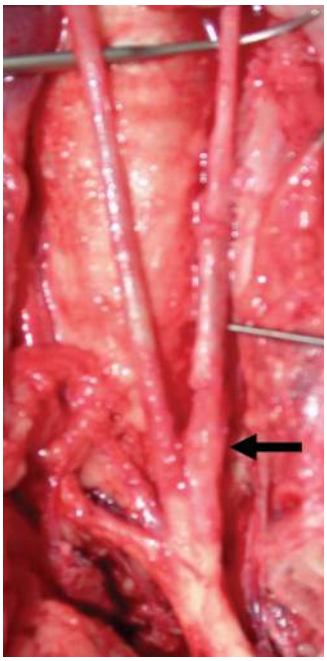

Figure 7. Gross necropsy of a successfully recanalized CTO demonstrates proximal LCA thickening (black arrow) with no extramural injury.

atrial transseptal puncture.[16,19] CTO recanalization is a more complex procedure because the vascular lumen is smaller, the diseased vessels tend to be tortuous, and the risk of lethal perforation is higher when catheters are manipulated within the high-pressure arterial system. These support the principle that MRI has potential utility to guide conventional and novel catheter-based interventions because of superior tissue visualization.

Because the SNR of proton MRI is very low, there is inadequate temporal and spatial resolution to image coronary arteries in real-time with the use of MRI. Barring unforeseen technical breakthroughs, it is unlikely that such recanalization procedures can be conducted on occluded coronary arteries.

Limitations

The comparison of x-ray– and MRI-guided recanalization attempts should be interpreted with caution because of the imbalance in the number of animals in each group and because primary and crossover attempts were combined for analysis.

Repeated use of recycled devices, abrupt transition points, high friction, and poor mechanical responsiveness account for failure to recanalize and deliver catheter devices into the target arterial occlusion in a few animals. Our homemade devices had inferior capacity for pushing, torque, and tip-bending performance compared with clinical x-ray devices in bench testing (data not shown). Low-profile, tapered, trackable, steerable, and hydrophilic-coated active MRI devices can be manufactured with available technology but would have been prohibitively expensive to manufacture in the small quantities tested here. In addition, suitable stents would have treated flow-limiting artery recoil and spasm but were not used here. Metal alloys such as nitinol, platinum-iridium, or nickel-cobalt-chromium have less MRI susceptibility artifact than stainless steel. Numerous reports already have been published of experimental rtMRI-guided deployment of such devices.[7,17,18,45] Nevertheless, our primary end point, rtMRI-guided CTO recanalization, was successfully accomplished with the use of our rudimentary device prototypes. Subsequent therapy to maintain antegrade flow and patency such as stenting could be conducted under x-ray, immediately after successful rtMRI CTO recanalization.

Conclusions

This work demonstrates the feasibility of rtMRI guidance to recanalize arterial CTO with the use of custom active MRI visible devices in a suitably challenging swine model. Future image-guided human peripheral artery CTO interventions may be possible with the use of this technology. However, clinical-grade catheter devices must be manufactured to translate these findings into patients.

Acknowledgments

This study was supported by National Institutes of Health grant Z01-HL005062-03 (Dr Lederman). The authors thank Kathryn Hope, Kathy Lucas, and Joni Taylor for their animal care and support.

Disclosures

None.

References

1. Management of peripheral arterial disease (PAD): TransAtlantic Inter-Society Consensus (TASC), section B: intermittent claudication. *J Vasc Surg*. 2000;31(pt 2):S54–S134.
2. Management of peripheral arterial disease (PAD): TransAtlantic Inter-Society Consensus (TASC), section D: chronic critical limb ischaemia. *J Vasc Surg*. 2000;31(pt 2):S168–288.
3. Yang X, Bolster BD Jr, Kraitchman DL, Atalar E. Intravascular MR-monitored balloon angioplasty: an in vivo feasibility study. *J Vasc Interv Radiol*. 1998;9:953–959.
4. Guttman MA, Lederman RJ, Sorger JM, McVeigh ER. Real-time volume rendered MRI for interventional guidance. *J Cardiovasc Magn Reson*. 2002;4:431–442.
5. Lardo AC, McVeigh ER, Jumrussirikul P, Berger RD, Calkins H, Lima J, Halperin HR. Visualization and temporal/spatial characterization of cardiac radiofrequency ablation lesions using magnetic resonance imaging. *Circulation*. 2000;102:698–705.
6. Bartels LW, Bos C, van Der Weide R, Smits HF, Bakker CJ, Viergever MA. Placement of an inferior vena cava filter in a pig guided by high-resolution MR fluoroscopy at 1.5 T. *J Magn Reson Imaging*. 2000;12:599–605.
7. Manke C, Nitz WR, Djavidani B, Strotzer M, Lenhart M, Volk M, Feuerbach S, Link J. MR imaging-guided stent placement in iliac arterial stenoses: a feasibility study. *Radiology*. 2001;219:527–534.
8. Buecker A, Spuentrup E, Grabitz R, Freudenthal F, Muehler EG, Schaeffter T, van Vaals JJ, Gunther RW. Magnetic resonance-guided placement of atrial septal closure device in animal model of patent foramen ovale. *Circulation*. 2002;106:511–515.
9. Rickers C, Jerosch-Herold M, Hu X, Murthy N, Wang X, Kong H, Seethamraju RT, Weil J, Wilke NM. Magnetic resonance image-guided transcatheter closure of atrial septal defects. *Circulation*. 2003;107:132–138.
10. Schalla S, Saeed M, Higgins CB, Martin A, Weber O, Moore P. Magnetic resonance–guided cardiac catheterization in a swine model of atrial septal defect. *Circulation*. 2003;108:1865–1870.
11. Dick AJ, Guttman MA, Raman VK, Peters DC, Pessanha BS, Hill JM, Smith S, Scott G, McVeigh ER, Lederman RJ. Magnetic resonance fluoroscopy allows targeted delivery of mesenchymal stem cells to infarct borders in Swine. *Circulation*. 2003;108:2899–2904.
12. Razavi R, Hill DL, Keevil SF, Miquel ME, Muthurangu V, Hegde S, Rhode K, Barnett M, van Vaals J, Hawkes DJ, Baker E. Cardiac cath-

eterisation guided by MRI in children and adults with congenital heart disease. *Lancet*. 2003;362:1877–1882.
13. Kuehne T, Yilmaz S, Meinus C, Moore P, Saeed M, Weber O, Higgins CB, Blank T, Elsaesser E, Schnackenburg B, Ewert P, Lange PE, Nagel E. Magnetic resonance imaging-guided transcatheter implantation of a prosthetic valve in aortic valve position: feasibility study in swine. *J Am Coll Cardiol*. 2004;44:2247–2249.
14. Kee ST, Ganguly A, Daniel BL, Wen ZBS, Butts K, Shimikawa A, Pelc NJ, Fahrig R, Dake M. MR-guided transjugular intrahepatic portosystemic shunt creation with use of a hybrid radiography/MR system. *J Vasc Interv Radiol*. 2005;16:227–234.
15. Schalla S, Saeed M, Higgins CB, Weber O, Martin A, Moore P. Balloon sizing and transcatheter closure of acute atrial septal defects guided by magnetic resonance fluoroscopy: assessment and validation in a large animal model. *J Magn Reson Imaging*. 2005;21:204–211.
16. Arepally A, Karmarkar PV, Weiss C, Rodriguez ER, Lederman RJ, Atalar E. Magnetic resonance image-guided trans-septal puncture in a swine heart. *J Magn Reson Imaging*. 2005;21:463–467.
17. Raman VK, Karmarkar PV, Guttman MA, Dick AJ, Peters DC, Ozturk C, Pessanha BS, Thompson RB, Raval AN, DeSilva R, Aviles RJ, Atalar E, McVeigh ER, Lederman RJ. Real-time magnetic resonance-guided endovascular repair of experimental abdominal aortic aneurysm in swine. *J Am Coll Cardiol*. 2005;45:2069–2077.
18. Raval AN, Telep JD, Guttman MA, Ozturk C, Jones M, Thompson RB, Wright VJ, Schenke WH, Desilva R, Aviles RJ, Raman VK, Slack MC, Lederman RJ. Real-time magnetic resonance imaging–guided stenting of aortic coarctation with commercially available catheter devices in swine. *Circulation*. 2005;112:699–706.
19. Raval AN, Karmarkar PV, Guttman MA, Ozturk C, DeSilva R, Wright VJ, Schenke WH, Atalar E, McVeigh ER, Lederman RJ. Real-time MRI guided atrial septal puncture and balloon septostomy in swine. *Cathet Cardiovasc Interv*. In press.
20. Dick AJ, Raman VK, Raval AN, Guttman MA, Thompson RB, Ozturk C, Peters DC, Stine AM, Wright VJ, Schenke WH, Lederman RJ. Invasive human magnetic resonance imaging: feasibility during revascularization in a combined XMR suite. *Catheter Cardiovasc Interv*. 2005;64:265–274.
21. Ocali O, Atalar E. Intravascular magnetic resonance imaging using a loopless catheter antenna. *Magn Reson Med*. 1997;37:112–118.
22. Atalar E. Radiofrequency safety for interventional MRI procedures (1). *Acad Radiol*. 2005;12:1149–1157.
23. Yeung CJ, Susil RC, Atalar E. RF safety of wires in interventional MRI: using a safety index. *Magn Reson Med*. 2002;47:187–193.
24. Preacher K, Briggs N. Interactive Fisher's exact test. Available at: http://www.unc.edu/~preacher/fisher/fisher.htm. Accessed October 28, 2005.
25. Johnston KW. Iliac arteries: reanalysis of results of balloon angioplasty. *Radiology*. 1993;186:207–212.
26. Reyes R, Maynar M, Lopera J, Ferral H, Gorriz E, Carreira J, Castaneda WR. Treatment of chronic iliac artery occlusions with guide wire recanalization and primary stent placement. *J Vasc Interv Radiol*. 1997;8:1049–1055.
27. Uher P, Nyman U, Lindh M, Lindblad B, Ivancev K. Long-term results of stenting for chronic iliac artery occlusion. *J Endovasc Ther*. 2002;9:67–75.
28. Steinkamp H, Werk M, Wissgott C, Settmacher U, Haufe M, Hierholzer C, Felix R. Stent placement in short unilateral iliac occlusion: technique and 24-month results. *Acta Radiol*. 2001;42:508–514.
29. Gupta AK, Ravimandalam K, Rao VR, Joseph S, Unni M, Rao AS, Neelkandhan KS. Total occlusion of iliac arteries: results of balloon angioplasty. *Cardiovasc Intervent Radiol*. 1993;16:165–177.
30. Carnevale FC, De Blas M, Merino S, Egana JM, Caldas JG. Percutaneous endovascular treatment of chronic iliac artery occlusion. *Cardiovasc Intervent Radiol*. 2004;27:447–452.
31. Blum U, Gabelmann A, Redecker M, Noldge G, Dornberg W, Grosser G, Heiss W, Langer M. Percutaneous recanalization of iliac artery occlusions: results of a prospective study. *Radiology*. 1993;189:536–540.
32. Dyet JF, Gaines PA, Nicholson AA, Cleveland T, Cook AM, Wilkinson AR, Galloway JM, Beard J. Treatment of chronic iliac artery occlusions by means of percutaneous endovascular stent placement. *J Vasc Interv Radiol*. 1997;8:349–353.
33. Vorwerk D, Guenther RW, Schurmann K, Wendt G, Peters I. Primary stent placement for chronic iliac artery occlusions: follow-up results in 103 patients. *Radiology*. 1995;194:745–749.
34. Ashley S, Brooks SG, Gehani AA, Kester RC, Rees MR. Percutaneous laser recanalisation of femoropopliteal occlusions using continuous wave Nd-YAG laser and sapphire contact probe delivery system. *Eur J Vasc Surg*. 1994;8:494–501.
35. Lofberg AM, Karacagil S, Ljungman C, Westman B, Bostrom A, Hellberg A, Ostholm G. Percutaneous transluminal angioplasty of the femoropopliteal arteries in limbs with chronic critical lower limb ischemia. *J Vasc Surg*. 2001;34:114–121.
36. Perin EC, Sarmento-Leite R, Silva GV, Rogers MD, Topaz O. "Wireless" laser recanalization of chronic total coronary occlusions. *J Invas Cardiol*. 2001;13:401–405.
37. Scheinert D, Laird JR, Jr., Schroder M, Steinkamp H, Balzer JO, Biamino G. Excimer laser-assisted recanalization of long, chronic superficial femoral artery occlusions. *J Endovasc Ther*. 2001;8:156–166.
38. Yamashita T, Kasaoka S, Son R, Gordon IL, Khan R, Neet J, Hedrick AD, Tobis JM. Optical coherent reflectometry: a new technique to guide invasive procedures. *Cathet Cardiovasc Interv*. 2001;54:257–263.
39. Mossop P, Cincotta M, Whitbourn R. First case reports of controlled blunt microdissection for percutaneous transluminal angioplasty of chronic total occlusions in peripheral arteries. *Cathet Cardiovasc Interv*. 2003;59:255–258.
40. Coggia M, Javerliat I, Di Centa I, Colacchio G, Leschi JP, Kitzis M, Goeau-Brissonniere OA. Total laparoscopic bypass for aortoiliac occlusive lesions: 93-case experience. *J Vasc Surg*. 2004;40:899–906.
41. Casserly IP, Sachar R, Bajzer C, Yadav JS. Utility of IVUS-guided transaccess catheter in the treatment of long chronic total occlusion of the superficial femoral artery. *Cathet Cardiovasc Interv*. 2004;62:237–243.
42. Yang YM, Mehran R, Dangas G, Reyes A, Qin J, Stone GW, Leon MB, Moses JW. Successful use of the frontrunner catheter in the treatment of in-stent coronary chronic total occlusions. *Cathet Cardiovasc Interv*. 2004;63:462–468.
43. Kawarada O, Yokoi Y, Morioka N, Nakata S, Takemoto K. Chronic total occlusions in the superficial femoral artery: a novel strategy using a 1.5 mm J-tip hydrophilic guidewire with an over-the-wire balloon catheter under ultrasound guidance. *Cathet Cardiovasc Interv*. 2005;65:187–192.
44. Kee ST, Rhee JS, Butts K, Daniel B, Pauly J, Kerr A, O'Sullivan GJ, Sze DY, Razavi MK, Semba CP, Herfkens RJ, Dake MD. 1999 Gary J. Becker Young Investigator Award: MR-guided transjugular portosystemic shunt placement in a swine model. *J Vasc Interv Radiol*. 1999;10:529–535.
45. Kuehne T, Saeed M, Higgins CB, Gleason K, Krombach GA, Weber OM, Martin AJ, Turner D, Teitel D, Moore P. Endovascular stents in pulmonary valve and artery in swine: feasibility study of MR imaging-guided deployment and postinterventional assessment. *Radiology*. 2003;226:475–481.

CLINICAL PERSPECTIVE

Traditionally, surgical bypass is preferred over x-ray–guided endovascular repair for long, tortuous chronic total occlusion (CTO). Endovascular guidewire traversal under x-ray is conducted almost "blindly" through occluded vessels that are not opacified by contrast. The guidewires and catheters required to recanalize these lesions risk failure, perforation, and life-threatening hemorrhage. We demonstrate successful real-time MRI-guided recanalization of a long peripheral artery CTO in a suitable pig model. Real-time MRI may offer an advantage in artery visualization during CTO traversal while obviating ionizing radiation and nephrotoxic radiocontrast.

APPENDIX: Custom Active Chronic Total Occlusion Device Heat Testing

Device heat tests were performed on the active guidewire and the catheter in a 20 cm diameter, 70 cm long polyacrylamide gel (PAG) phantom according to previously described methods.[27] PAG has conductivity similar to that of human tissue (0.7 siemens/meter at 64 MHz). The heating tests were performed using a steady state free precession pulse sequence with a peak whole body SAR of 4 W/kg. Duringc10 to 20 minutes of continuous scanning, local temperature changes at various sections along the device length were recorded using fiberoptic temperature probes (UMI4; FISO Technologies). SAR was calculated by multiplying the slope of temperature rise (dT/dt) with specific heat of the gel (4180 J/kg). Five probes were positioned adjacent to key points along the active device. (Catheter: at the distal catheter tip, middle of loop coil, proximal end of loop coil, the distal end of the braid and 20 cm proximal to the distal end of the catheter; Guidewire: distal tip, middle of loop, proximal end of loop, middle of MP35N coil, proximal end of coil and 20 cm from the distal end. Combination guidewire/catheter was tested with wire extending 1.5 cm outside catheter. Probes were placed at: distal end of wire, distal end of guide (middle of the guidewire loop), middle of catheter loop, proximal end of catheter loop, distal end of catheter braid. For maximum energy deposition, the guidewire and the catheter were placed 2 cm from the phantom edge placed 10 cm off magnet isocenter.

Results: Heat tests for device safety are summarized in the Table. The maximum SAR was observed at the middle of the catheter loop. When guidewire and catheter were combined, the local SAR was close to the sum of the local SARs of the two devices. The minor temperature elevations associated with each device location (<2 ^{o}C) would not be expected to result in tissue damage or adverse effects based on these conditions.

Conclusions: These custom active guidewires and catheter do not heat significantly under these test conditions.

Appendix Table: Local temperature changes during 10 minute test scan

Guiding catheter					
Location	**Distal Tip**	**Mid Loop**	**Proximal loop**	**Distal end of braid**	**20 cm from tip**
SAR	4.0 W/kg	6.0 W/kg	10.0 W/kg	1.2 W/kg	3.5 W/kg
Temp rise	0.1 ^{o}C	0.4^{o}C	0.6 ^{o}C	0.2 ^{o}C	0.2 ^{o}C

Guidewire					
Location	**Distal Tip**	**Mid Loop**	**Proximal loop**	**Mid MP35N coil**	**Proximal end of MP35N coil**
SAR	11 W/kg	5.0 W/kg	2.0 W/kg	19.0 W/kg	6.0 W/kg
Temp rise	0.2 ^{o}C	0.1 ^{o}C	0.1 ^{o}C	0.4 ^{o}C	0.2 ^{o}C

Guidewire Inside Guiding Catheter (Combined)					
Location	**Distal Tip of wire**	**Distal Tip of catheter**	**Mid Loop catheter**	**Distal end of braid catheter**	**20 cm proximal from tip of wire**
SAR	8 W/kg	21 W/kg	26 W/kg	5 W/kg	5 W/kg
Temp rise	0.7^{o}C	1.3 ^{o}C	1.4 ^{o}C	0.9 ^{o}C	0.4 ^{o}C